

## Intrinsic Classification of Single Particle Images by Spectral Clustering

Yutaka Ueno<sup>1</sup>, Masaki Kawata<sup>2</sup> and Shinji Umeyama<sup>1</sup>

<sup>1</sup> Neuroscience Research Institute,  
<sup>2</sup> Grid Technology Research Center,  
National Institute of Advanced Industrial Science and Technology, 1 Umezono Central-2,  
Tsukuba, 305-8568, Japan  
uenoyt@ni.aist.go.jp,  
{m.kawata,s.umeyama}@aist.go.jp

**Abstract.** An application of spectral clustering to single particle analysis of a biological molecule is described. Using similarity scores for the given data set, clustering was performed in a factor space made by the eigenvector of the normalized similarity matrix. Image data was thus classified by means of information intrinsic to the ensemble of given data. The method was tested on a simulated transmission electron microscopy image and a real image data set of 70S ribosome. The average images of clusters were obtained by iterative alignment, which successfully represented characteristic views of the target molecules. Comparisons with traditional methods and techniques in practical implementation are discussed.

### 1 Introduction

With the increasing attention given to single particle analysis for structural analysis of biological molecules, novel classification algorithms and mathematical studies are in demand for automated image processing. A currently popular image processing method first tries to align all images in rotation and translations, then performs multivariate statistic analysis — in particular, correspondence analysis — to classify images into sub classes [1]. Then, images for a class are searched from the whole set of images and the members of the class refined. This process is called multi-reference alignment. While many studies in structural biology have benefited from this method, very careful assessment of classification results are required [2].

Unfortunately, the obtained class average images are often not sufficient for subsequent structural analysis of the molecule. Under the minimum dose condition in transmission electron microscopy, the obtained images are immersed in substantial background noise, and image alignment is a critical step [1]. Although a reference free alignment [3] was proposed to align images without prior knowledge of the particle structure, the classification task is hardly trivial. Invariant classification [4] also addresses this problem of unsupervised clustering; however, its performance is insufficient for wider application in this field [5].

In contrast, data mining studies — for example, information discovery in large text database and trade information database systems — have researched various

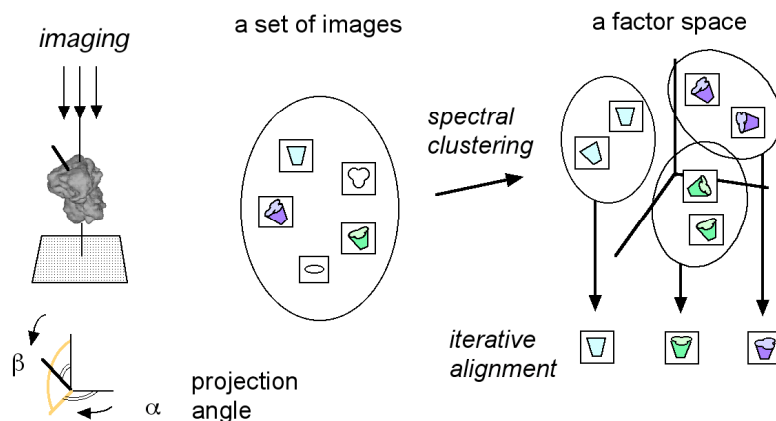


**Fig. 1.** Overview of single particle analysis with spectral clustering. Similar pairs of images are mapped in near locations on a factor space

algorithms to meet the emerging demand. Spectral clustering [6], which groups data by an eigenvalue method, has demonstrated advanced performance in text data clustering [7] and image segmentation problems [8]. The kernel principal component analysis [9] which has been developed differently, shares the same concept of eigenvalue solutions, emphasizing the efficiency of the nonlinear kernel function introduced to the distance measure for the observed data set.

In this paper, we consider the unsupervised clustering<sup>1</sup> of molecular images for alignment within a consistent set group. Instead of a reference-based method, which involves potential bias to preferences, we have applied spectral clustering, and evaluated its performance with simulated transmission electron microscope images and a data set from a real observation. Our results illustrate that appropriate groups are resolved through intrinsic classification of images with a common motif. We also discuss a mechanism for clustering images and indispensable techniques in practical implementations for single particle analysis.

Fig. 1 illustrates an overview of single particle analysis with spectral clustering. Digitized micrographs are windowed into individual particle images. Noise must then be reduced by averaging images, grouping and alignment of images. Spectral clustering involves mapping images onto a factor space, which is different from one used in correspondence analysis [10], then the images are grouped by means of their coordinates. The obtained images in a group are aligned and averaged by the iterative alignment method [3].

## 2 Method

### 2.1 Spectral Clustering

<sup>1</sup> The word "clustering" is used for unsupervised grouping, while "classification" implies supervised grouping of a data set.

Below are the steps for the Ng-Jordan-Weiss algorithm [6] for spectral clustering of  $k$  subsets for a given set of points  $S=\{s_1, s_2, \dots, s_n\}$  in  $\mathbb{R}^n$  :

1. From the similarity matrix<sup>2</sup>  $\mathbf{A}$  in  $\mathbb{R}^{n \times n}$  defined by  $A_{ij} = \exp(-\|s_i - s_j\|^2 / \sigma^2)$  for  $i \neq j$  and  $A_{ii} = 0$ .
2. Define  $\mathbf{D}$  to be the diagonal matrix with  $D_{ii} = \sum_{j=1, n} A_{ij}$
3. Normalize  $\mathbf{N} = \mathbf{D}^{-1/2} \mathbf{A} \mathbf{D}^{-1/2}$
4. Find  $x_1, x_2, \dots, x_k$  the  $k$  largest eigenvectors of  $\mathbf{N}$  and form the matrix  $\mathbf{X} = [x_1, x_2, \dots, x_k]$
5. Normalize the rows of  $\mathbf{X}$  to be of unit length
6. Treating each row of  $\mathbf{X}$  as a point in  $\mathbb{R}^k$ , cluster into  $k$  clusters using k-means or any other sensible clustering algorithm.
7. Assign the original point  $s_i$  to cluster  $j$  if and only if row  $i$  of  $\mathbf{X}$  was assigned to cluster  $j$ .

The scaling parameter  $\sigma$  controls how rapidly the similarity values fall off. There are other studies for normalization step 3, which can adapt to individual problems [7].

## 2.2 A Fast Calculation of Similarity Between Images

The cross correlation of images is used for the similarity measure between images. The similarity of two images,  $x$  and  $y$ , is evaluated by maximizing the cross correlation in rotation  $R$  and translation  $t$  of image  $y$ .

$$Crr(x, y) = \sum_i^{pixels} (x_i - \bar{x})(y_i - \bar{y}) / \sigma_x \sigma_y \quad (1)$$

$$c_{xy} = \max_{R, t} Crr(x, T(y; R, t)) \quad (2)$$

$x_i$  is the  $i$ -th pixel of image  $x$ ;  $\bar{x}$  and  $\sigma_x$  is the mean and the standard deviation of image  $x$ ;  $T(y; R, t)$  designates the transformed image. Then, the similarity matrix is defined as follows.

$$A_{xy} = \exp((1 - c_{xy}) / \sigma^2) \quad (3)$$

Spectral clustering requires these distance values between all pairs of images with the best matching rotation and translations, that distinguish our method from the traditional method. Since it requires extensive computation, we devised a fast calculation method. Both rotation and translation searches are performed in two steps, coarse and fine. In addition, a table of pixels addressing all pixels and rotation angles is pre-calculated to reduce computation.

## 2.3 Dimension Reduction of Similarity Matrix

For very large numbers of images the calculation of a similarity matrix is overwhelmed by the vast number of image-pair similarity scores. There are ways to

---

<sup>2</sup> The term “affinity matrix” in the original paper was superseded by “similarity matrix” because the former term was confusing in the field of molecular biology.

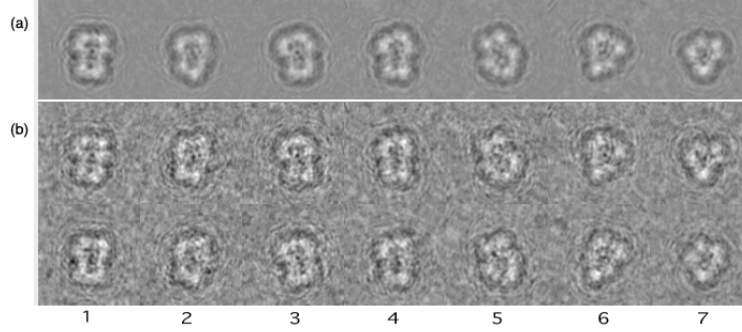


**Fig. 2.** Clustering result for simulated images of the blue tongue virus coat protein trimer. Seven groups except three mirror images for 2,3,4 are depicted. (a) average images for each clusters (b) two sample images assigned to each clusters

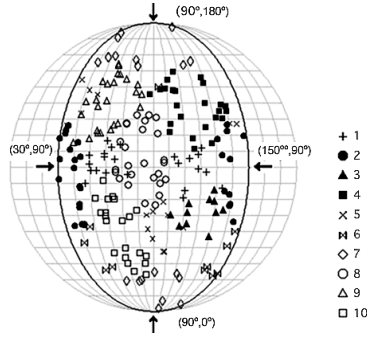


**Fig. 3.** The distribution of the predefined projection angles ( $\alpha, \beta$ ) of individual images in obtained clusters. With three fold symmetry of this particle, projection angles were limited between 30 and 150 for  $\alpha$

reduce the dimensions of the similarity matrix, however. For example, random selection of images is sufficient in most cases for the first step of clustering images.

In addition, a significant portion of the similarity matrix can be estimated. For example, eliminating odd images is a conventional method, which usually gives a low correlation value to any of good images. The average correlation to randomly selected images is useful to rank images and find odd images.

### 3 Results

#### 3.1 Test with Simulated Images

In order to evaluate the performance of spectral clustering, we first applied it to simulated projection images for transmission electron microscopy of a protein. A trimer of blue tongue virus coat protein was chosen as well as a sample data set in EMAN software [19]. Volume density was calculated from the atomic coordinates data entry 1BTB in the protein databank. Using random projection angles, a total of 300 of synthetic images with size 100x100 was processed by the contrast transfer function filter [5], and random noises were added.

Fig. 2 illustrates the cluster images obtained by averaging images of the clusters

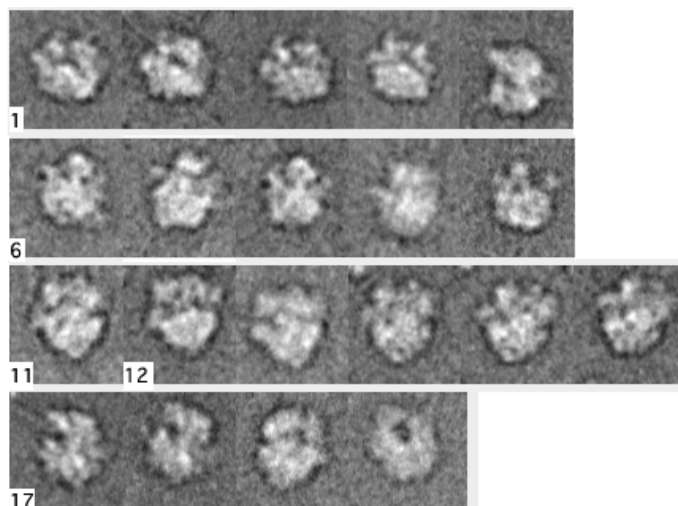


**Fig. 4.** The cluster average images of 70S *ecoli* ribosome [11] obtained by our spectral clustering. Orientations of images are roughly adjusted to demonstrates similar views of particle orientations, The top line lists five images small and globular; the second line showed the famous portrait of the ribosome; in the third line particles look larger; and the fourth line are the others

with iterative alignment, and their member images. The common image features among the cluster images were successfully extracted. Fig. 3 shows a distribution of cluster members in the projection angle of individual images. Due to the three-fold symmetry of the molecule, the imposed cluster number 10 seemed to be adequate to distinguish classes of images. The scaling parameter was set to  $\sigma=1/\sqrt{2}$ .

### 3.2 Test with Ribosome Images

Among successful results in application to real data set from transmission electron microscopy, we demonstrate a result of 70S ribosome by cryo-electron microscopy [11], which is provided by SPIDER software package [17] including the three-dimensional volume data reconstructed from the data set; therefore, it allows us to evaluate the results of clustering performance by comparisons with the projection of the volume at various angles (Fig. 5c).

At first, odd images without particle images were eliminated from the 6996 total images. The result of spectral clustering using 700 randomly selected images with size 75x75 to form 20 clusters, with the scaling parameter  $\sigma=0.5$ , is illustrated in Fig. 4. The iterative alignment of the obtained cluster images nicely exhibited most characteristic views of the ribosome published by the original study [11]. Different values of the scaling parameter and various calculation methods for similarity matrix were also tested, but results were similar and less distinct.

From raw images of the cluster members, it was difficult for the images to be classified by hand (Fig. 5a). In addition, we failed reproduce the original result by means of traditional method on software package IMAGIC [18]. Using the obtained

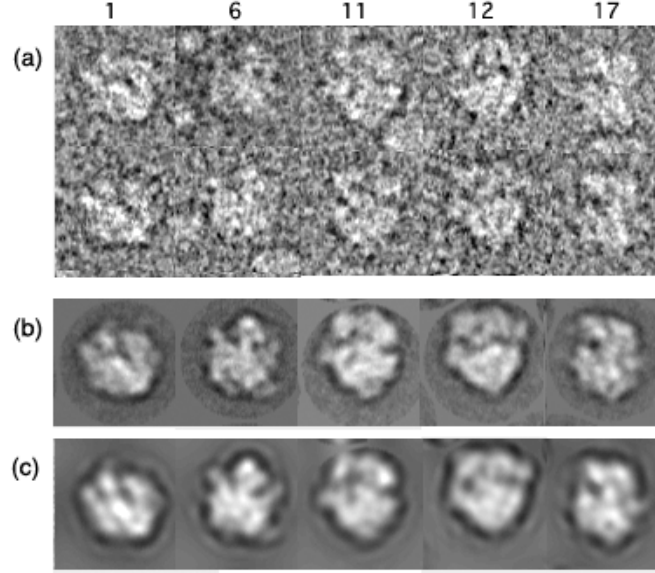


**Fig. 5.** (a) Raw images for selected distinct clusters in Fig. 4. (b) The average images refined by multi-reference alignment against the whole image data set. (c) Corresponding projection images of the volume data after a final refinement of three dimensional reconstruction

cluster images as seed images, similar images were searched in the observed images by means of multi-reference alignment. The result improved the resolution of the average image (Fig. 5b). They were consistent to the projection images from the three dimensional reconstruction (Fig. 5c). Thus, it seems to be satisfactory for the subsequent three-dimensional reconstruction, indicating that clusters had been resolved appropriately.

While clustering results are usually checked by the resolution assessment such as Fourier shell correlation [1], we tried to estimate projection angles of the observed images from a reference volume of the structure. However, they were too noisy to confirm their accuracy. The distribution of estimated projection angles showed less clear separation of clusters than was the case with the previous test (Fig.3). Many clusters occupied two different regions in the projection angle coordinates, which also correspond to a pseudo mirror symmetry of the image.

## 4 Discussion and Conclusion

### 4.1 Comparison with the Traditional Method

The traditional method of correspondence analysis [12] takes a vector of the image pixel; then clustering results also provide information about important pixels, which is

used as a mask to improve classification. With this method, small differences between projection images were superbly clarified [13]. However, particle images with various orientations are difficult to align in general, and the subsequent supervised classification by preferred seed images tends to fail. In this procedure, we need to align images to produce trends of classification. Moreover, images with different features, for example, a top view and side views of the molecule, are all compared in a single alignment, so that it is easy to encounter an artifact image.

We consider that images with different features should be separated in the traditional framework with multivariate statistic analysis using aligned images. The features of images should be resolved intrinsically from the context of the image ensemble. Spectral clustering is an algorithm for addressing this kind of problem.

## 4.2 Mechanism of Clustering

Spectral clustering only takes into account distances within data sets, once the pixel data have been used to construct the similarity matrix. One worries that a single similarity value between two images provides little information as to the optimum image alignment, and that it can be disturbed by noise. However, on the other hand, there are other similarity values against other images which support the trend of clustering from different points of view.

Therefore, once several images are found with very high similarity, and they are confirmed as different from other images, they obtain a certain magnitude in factor coordinates to be distinguished as a cluster. The factor space is constructed by the eigenvector of normalized similarity matrix. The vector is not directly calculated from pixels of a single image, but defined as the mutual relationship of images within the ensemble of the data set. Images can be located at a position in space constructed by cooperation of all image data, ensuring an unsupervised method of clustering. Using this factor space, the distance of images becomes Euclidian, which is required for stable convergence in the k-means algorithm [14].

## 4.3 Techniques in Practical Implementation

In our framework of spectral clustering, the calculation of a similarity matrix requires extensive computation, which had been a disadvantage in comparison to other methods [5]. However, our fast implementation allowed performance improvements in feasible degrees on current microprocessors. For example, it takes about 45 minutes for 700 images of size 75x75 on a 3GHz Pentium4 (Intel Corp.). Besides our code, there are ways to accelerate computations [15].

The accurate evaluation of similarity is key to the successful clustering of noisy images, even though the dimension of the similarity matrix is reduced. Besides random sampling of images, we can rank images so that significant images will represent the most important part of the whole similarity matrix.

We demonstrated our successful results with spectral clustering for intrinsic classification of single particle images. To establish a robust software system, the scaling parameter of spectral clustering and other options need to be optimized. Moreover, a learning algorithm to automate the parameter tuning [7],[8] is also an intriguing topic for the future development of our software system [16].

## Acknowledgement

The authors would like to thank Dr. Patrick Schultz, Dr. Bruno P. Klaholz and Dr. Dino Moras at IGBMC/University Louis Pasteur for their helpful discussions. We are greatly encouraged by Dr. Andreas Engel and Dr. Chikara Sato. In this study we used electron microscopy images of the 70S ribosome, distributed with the software package SPIDER, with kind permission by Dr. Joachim Frank.

## References

1. Frank, J.: Three-Dimensional Electron Microscopy of Macromolecular Assemblies, Academic Press. (1996)
2. Ueno, Y., Sato, C.: Three-dimensional Reconstruction of Single Particle Electron Microscopy: the Voltage Sensitive Sodium Channel Structure. *Science Progress* **84** (2002) 291-309
3. Penczek, P.A., Grassucci, R.A., Frank, J.: Three-dimensional Reconstruction of Single Particles Embedded in Ice. *Ultramicroscopy* **40** (1992) 33-53
4. Schatz, M., van Heel, M.: Invariant Recognition of Molecular Projections in Vitreous Ice Preparations. *Ultramicroscopy* **45** (1992) 15-22
5. Joyeux, L., Penczek, P.A.: Efficiency of 2D alignment methods, *Ultramicroscopy* **92** (2002) 33-46
6. Ng, A., Jordan, M.I., Weiss, Y.: On spectral Clustering: Analysis and an algorithm. In *advances in Neural Information Processing Systems* **14** (2001)
7. Kamvar, S.D., Klein, D., Manning, C.D.: Spectral Learning. *Proceedings of the Eighteenth International Joint Conference on Artificial Intelligence* (2003) pp.561-566
8. Zelnik-Manor, L., Perona, P.: Self-Tuning Spectral Clustering. In *advances in Neural Information Processing Systems* **17** (2004)
9. Scholkopf, B., Smola, A., Muller, K.-R.: Nonlinear Component Analysis as a Kernel Eigenvalue Problem. *Neural Computation* **10** (1998) 1299-1319
10. van Heel, M.: Classification of Very Large Electron Microscopical Image Data Sets. *Optik* **82** (1989) 114-126
11. Penczek, P.A., Grassucci, R.A., Frank, J.: The Ribosome at Improved Resolution: New Techniques for Merging and Orientation Refinement in 3D cryo-electron Microscopy of Biological Particles. *Ultramicroscopy* **53** (1994) 251-270
12. Frank, J. and Voublik, M.: Multivariate Statistical Analysis of Ribosome Electron Micrographs. *Journal of Molecular Biology* **161** (1982) 117-137
13. Bruno, P.K., Pape, T., Zavialov, V., Myasnikov, A.G., Orlova, E.V., Vestergaard, B., Ehrenberg, M., vanHeel, M.: Structure of the Escherichia coli ribosomal termination complex with release factor 2. *Nature* **421** (2003) 90-94
14. Asai, K., Ueno, Y., Sato, C. and Takahashi, K.: Clustering and Averaging of Image in Single-particle Analysis. *Genome Informatics*, **11** (2000) 151-160
15. Cong, Y., Kovacs, J.A., Wriggers, W.: 2D fast rotational matching for image processing of biophysical data. *Journal of Structural Biology* **144** (2003) 51-60
16. Ueno, Y., Takahashi, K., Asai, K., Sato, C.: BESPA: Software Tools for Three-dimensional Structure Reconstruction From Single Particle Images of Proteins. *Genome Informatics* **10** (1999) 241-242; on the web <http://moonscript.net/bespa/>
17. SPIDER software package. [http://wadsworth.org/spider\\_doc/](http://wadsworth.org/spider_doc/)
18. IMAGIC-V software package. <http://www.imagescience.de/>
19. EMAN software package. <http://ncmi.bcm.tmc.edu/~stevell/eman/doc/>